Topology optimization of piezoelectric sensors/actuators for torsional vibration control of composite plates

2006 Smart Mater. Struct. 15 253

(http://iopscience.iop.org/0964-1726/15/2/004)

INSTITUTE OF PHYSICS PUBLISHING SMART MATERIALS AND STRUCTURES
Smart Mater. Struct. **15** (2006) 253–269 doi:10.1088/0964-1726/15/2/004

Topology optimization of piezoelectric sensors/actuators for torsional vibration control of composite plates

S Y Wang[1], K Tai[2,4] and S T Quek[3]

[1] Centre for Singapore-MIT Alliance, National University of Singapore, E4-04-10, 4 Engineering Drive 3, 117576, Singapore
[2] School of Mechanical and Aerospace Engineering, Nanyang Technological University, 50 Nanyang Avenue, 639798, Singapore
[3] Department of Civil Engineering, National University of Singapore, 1 Engineering Drive 2, 117576, Singapore

E-mail: mktai@ntu.edu.sg

Received 3 November 2004, in final form 15 December 2005
Published 30 January 2006
Online at stacks.iop.org/SMS/15/253

Abstract
Torsional vibration control can be crucial for applications of smart materials and structures. In this paper, the problem of topology optimization of collocated piezoelectric sensor/actuator (S/A) pairs for torsional vibration control of a laminated composite plate is directly addressed. Both isotropic and anisotropic PZT S/A pairs are considered and it is highlighted that the torsional vibration can be more effectively damped out by employing the topological optimal design of the S/A pairs than by using the conventional designs. To implement this topology optimization, a genetic algorithm (GA) based on a bit-array representation method is presented and a finite element (FE) simulation model based on the first-order shear theory and an output feedback control law is adopted. Numerical experiments are used to verify the present algorithm and show that the present optimal topology design can achieve significantly better active damping effect than the one using a continuously distributed PZT S/A pair, which was often adopted by many other researchers. Together with the progress in laser cutting and micromachining techniques, topology optimization of piezoelectric sensors and/or actuators would be promising in active vibration control of smart structures.

(Some figures in this article are in colour only in the electronic version)

1. Introduction

Smart flexible structures often consist of thin components such as beams, plates and shells that have been fabricated from composite materials with interlayers of piezoelectric ceramic films. The use of composite materials in smart structures is especially interesting because of their potential for aeroelastic tailoring of the structure [1, 2]. The integration of composite structural design with an intelligent system would potentially enhance the performance of smart structures [3]. The promising potential of smart composite structures has triggered intense research interests, as reviewed in detail in [4–7]. In practice, two kinds of piezoelectric materials, the polyvinylidene fluoride (PVDF) polymer and the lead zirconate titanate (PZT) ceramic, have become most widely used in smart composite structures such as MEMS (micro-electro-mechanical systems) due to their light weight, relatively low cost, small size, and good frequency response.

As a sporadic problem in the industry for many years, torsional vibration is receiving more and more attention today as its serious durability effects become known and the maintenance costs would continue to grow. The topic

[4] Author to whom any correspondence should be addressed.

of torsional vibration could be crucial for some applications of smart materials and structures such as helicopter rotor blades [8] and thus appropriate methods to minimize this detrimental vibratory activity must be developed. The problem of torsional vibration control of smart composite structures with piezoelectric sensors and actuators has been studied by many researchers. Lee [9, 10] pointed out that only the PVDF polymer with a skew angle can sense and produce both bending and twisting motions in laminated plates due to its orthotropic nature and thus torsional vibration can be controlled. However, PVDF is compliant and thin and its electromechanical coupling coefficients are weak [3, 11] such that it is not a good actuator candidate for most engineering applications. In practice, the brittle and stiff PZT is most widely used as piezoelectric actuators due to its larger piezoelectric electromechanical coefficients. Park *et al* [12] has used the rectangular PZT patches attached on the host structure surfaces to produce bending and twisting motions to reduce the vibration. However, the rectangular PZT must have a high aspect ratio since it is assumed that it only induces strain in its longitudinal direction. It should be noted that, generally, a PZT actuator is naturally isotropic and it can only provide bending actuation [11] in 2D applications and the twisting motion may not be affected. Lee and Chan [13] studied the actuation mechanism of a torsional motion of laminated composite beams with a layer of embedded PZT and showed that the composite laminate can produce twisting deformation due to the existence of a coupling effect of the composite laminate. However, this twisting is secondary since it is only induced by the extension–twisting coupling. Aldraihem and Wetherhold [11] proposed a shear-deformable beam theory to model the coupled bending and twisting vibration in laminated beams. It was shown that the traditional PZT layers can detect and supply a twisting motion only indirectly while a PZT/epoxy composite (PZT/Ep) can sense and actuate both bending and twisting motions. Furthermore, it was reported that the PZT/Ep actuator can provide effective bending–twisting actuation for vibration damping. More recently, Zhu *et al* [14] presented a dynamic analytical model for torsional vibration induced by extension–twisting coupling of anisotropic composite laminates with piezoelectric actuators. The in-plane inertia was neglected and a reduced bending stiffness matrix was used. It was reported that this simplified model can provide a basis for analyzing some coupling vibration problems.

In practice, various applications of torsional vibration control of smart structures have also been well developed. Rodgers and Hagood [8] investigated the active twist control of the helicopter rotor blades using integrated active fiber composite (AFC) actuators as a means of reducing the detrimental torsional vibrations and noise. It was also illustrated that the active fiber composite material system can be tailored to achieve desired performance. Lee and Li [15] designed a rotary motor driven by an anisotropic composite lamina with piezoceramics as the actuator. Due to the material anisotropy and antisymmetric configuration, torsional vibration can be induced from the in-plane strain actuation. Rabinovitch and Vinson [16] proposed a systematic design approach for active piezoelectric fins developed for a small-scale flight vehicle. The piezoelectric twist actuator was designed to achieve enhanced performance and/or minimal power consumption by studying the influence of various parameters. However, the problem of optimal topological design of piezoelectric materials was not addressed in all these applications.

In optimal design of smart materials and structures, comprehensive reviews of the state of the art have been given by Frecker [5], as well as Padula and Kincaid [17]. According to Frecker [5], the ultimate goal in the development of optimization methods for smart structures is to devise a method to design actuators, sensors, structure, controller, and electronics simultaneously to work synergistically. However, due to the complexities of interactions involved, this problem is far from being solved [5, 18]. In the field of torsional or coupling vibration control of smart structures, the problem of optimal design of piezoelectric sensors and actuators has attracted the attention of a number of researchers. Burke and Hubbard's pioneer work [19] highlighted the importance of optimal configuration of piezoelectric materials since they found that a continuously distributed piezoelectric actuator with constant thickness bonded on the top surface of a simply supported beam cannot suppress some vibration modes. However, their work is limited to the design of the thickness of the continuously distributed piezoelectric material while shape and topology optimization methods, possibly more effective, were not introduced. Tzou and Fu [20] also illustrated that some vibration modes cannot be controlled by using fully distributed sensors and actuators due to the lack of observability and controllability. In their study, the fully distributed sensors and actuators were segmented into four pieces to control most vibration modes. Segmentations can be used to enhance control efficiency or to control several modes simultaneously [21]; however, the design process would become complex and the costs of the control system would increase as the number of segmented independent sensors and actuators increases. Therefore, research on optimal design of piezoelectric sensors and actuators, which guarantee more efficient use of piezoelectric materials, should be investigated. Hwang and Park [22] and Hwang *et al* [23] carried out research on optimal placement of the piezoelectric S/A pairs to suppress a torsional vibration mode of a composite plate. It was reported that the S/A pairs should be placed near the fixed boundary and away from the centerline of a cantilever plate to suppress the torsional vibration effectively. However, this observation was obtained from enumeration-based numerical experiments and more effective optimal search methods were not involved. Han and Lee [21] studied the problem of optimal placement of piezoelectric sensors and actuators using genetic algorithms (GAs) and significant vibration reduction for the first three vibration modes involving a torsional mode has been observed. Silva and Kikuchi [24] proposed a design method for piezoelectric transducers with specified frequencies and better performance characteristics based on topology optimization and the finite element method. Since the artificial material model [25] is used, a threshold value is used to reduce the amount of intermediate mass densities. However, it is not obvious how to define an appropriate threshold value to eliminate the gray scale of the final design. Li *et al* [26] studied the problem of optimal shape and location of piezoelectric materials for flextensional actuators by using

mixed variables and a GA. However, topology optimization of piezoelectric materials was not involved. Zhu *et al* [27] studied the optimal placement of PZT actuators for a plate structure under the action of bending and twisting loads. Although the optimal topology of the plate was found by using the popular power-law approach [28, 29], the shape and size of the actuator were pre-defined in their simultaneous optimal design. Quek *et al* [30] also studied the coupling vibration control of piezoelectric composite plates via the optimal placement of the S/A patches. It is shown that the optimal placement of isotropic PZT S/A patches, which agrees well with a simple prediction model, can damp out a torsional vibration mode effectively. However, the size of the rectangular patches is fixed and thus its efficiency may be further improved by using shape and topology optimization. Topology optimization of piezocomposites with optimal hydrophone characteristics was studied by Sigmund and Torquato [31], which is based on the SIMP (simple isotropic material with penalization) and sequential linear programming. More recently, Buehler *et al* [18] studied the problem of topology optimization of smart actuators based on the homogenization approach. Both the SIMP and the homogenization approach are based on the relaxation method [32] and thus a blurry boundary is evident in the final optimal design. Furthermore, optimal design of piezoelectric sensors and actuators for vibration control, which would be computationally more complex, was not addressed in these investigations.

Although there are numerous investigations and developments in modeling and optimization of torsional or coupling vibration control of smart structures, topology optimization of smart structures has been relatively less explored. As generally reviewed by Sigmund [33], the extensions of existing topology optimization methods for conventional materials to problems involving multiphysics and smart materials are relatively few. In most studies, configurations of piezoelectric sensors and actuators have been pre-specified. On the other hand, with the latest progress in laser cutting and micromachining techniques for hard and brittle materials, it has become possible to manufacture a piezoelectric sensor or actuator with complicated shape and topology. In [34], it was reported that the PZT ceramic can be cut using a high power laser to obtain very fine scale patterns. Hence, as indicated by Sigmund and Torquato [31] and Frecker [5], the development of topology optimization methods for smart materials and structures can be a promising new research area. It would thus be meaningful to carry out a further study on topology optimization of piezoelectric sensors/actuators for their effective applications in vibration control of smart composite plates.

The objective of the present study is to investigate topology optimization of a collocated piezoelectric S/A pair for effective torsional vibration control of a laminated composite plate. To model this torsional vibration control, an FE model [3, 35] using the first-order shear theory (FOST) and a simple output feedback control law are adopted. It is highlighted that the coupling effect of laminated composite plates would play a crucial role in torsional vibration control when isotropic PZT sensors/actuators are involved. To perform the topology optimization, a GA based on a bit-array representation method is further developed with desirable improvement in evolving connected topologies. Numerical examples illustrate that topology optimization of piezoelectric sensors/actuators can achieve significant improvement in damping out the torsional vibration and the numerical results can be well justified by the theoretical models for the sensing and actuation mechanisms. It should be noted that the proposed GA is applicable to a range of optimal design problems of smart structures where topology optimization of sensors and actuators is desirable, but the scope of this paper is to be limited to the two-dimensional problem of torsional vibration control of a composite plate for a full description of the present topology optimization algorithm.

2. Statement of the problem

Topology optimization can be considered as a generalized shape optimization method [25] and the topology optimization problem of finding the optimal material distribution is usually confined to a fixed reference (design) domain $\Omega \in \mathbb{R}^2$, which is bounded, open, and connected with Lipschitzian boundary $\partial\Omega$, to allow for the applied loads and boundary conditions [32]. The present topology optimization problem is to find the optimal material distribution of a surface-bonded collocated piezoelectric S/A pair such that the damping effect of the torsional vibration can be maximized. The design domain Ω is confined to the top (or bottom) surface of a laminated composite plate. The piezoelectric S/A pair is assumed to be collocated to guarantee the dynamic stability, as discussed in detail in [7]. In practice, the number of S/A pairs depends on many factors. As this number increases, the costs and weights of a control system will increase significantly [21]. It should also be noted that piezoelectric sensors/actuators are often applied to smart structures of small size. Hence, the difficulty in isolating the S/A pairs completely to achieve a high reliability will arise if multiple S/A pairs are used for a small size structure. In this study, only one or two S/A pairs are considered in the topology optimization for torsional vibration control, though the present algorithm can be applied to multiple S/A pairs. The present optimization problem can be mathematically expressed as

$$\begin{array}{lll} \max & f(\boldsymbol{x}), & \boldsymbol{x} \in \Omega \\ \text{s.t.}: & h_i(\boldsymbol{x}) = 0, & i = 1, 2, \ldots, I \\ & g_j(\boldsymbol{x}) \leqslant 0, & j = 1, 2, \ldots, J \end{array} \tag{1}$$

where $\boldsymbol{x}$ is the solution vector in the design domain Ω discretized by a fixed regular FE mesh, $f(\boldsymbol{x})$ the objective function to measure the damping effect, $h_i(\boldsymbol{x})$ the ith equality constraint function, I the total number of equality constraints, $g_j(\boldsymbol{x})$ the jth inequality constraint function, and J the total number of inequality constraints.

The original topology optimization problem formulated in equation (1) is a distributed, discrete valued design problem, or 0–1 problem [32]. Since binary variables can be used to indicate the presence or absence of material in the FE elements, it is very natural to adopt a bit-array representation (0–1 representation) method to define the topology of the S/A pairs. However, currently the most commonly used approach for the structural topology optimization problem is the relaxation method [25, 36], in which the binary variables of the original problem are relaxed and replaced with continuous variables to make full use of the well established continuous optimization

algorithms, such as the homogenization approach [37] or its alternative the SIMP (simple isotropic material with penalization) method [25, 28]. Although computationally effective, this method tends to converge to a local optimum and an optimal topology with blurry boundary or undesirable checkerboard patterns or an infeasible solution to the original 0–1 problem, as reported by some researchers [25, 32, 38–42].

In the present study, the original discrete optimization problem is solved directly by using the GA, which is a powerful and robust stochastic global search method first developed by Holland [43] and comprehensively studied by Goldberg [44]. The original infinite dimensional optimization problem which the discretized problem approximates may lack a solution in general since the set of feasible designs is not closed [32, 45]. To obtain a well posed problem, a restriction on the connectivity of the topology of each S/A pair is imposed in the present study to limit the geometric complexity of the structure and to prevent the occurrence of the checkerboard patterns (design restriction constraint). Typically this stochastic global search method would be computationally much more costly than a local search optimization method, but improvements in real computing time could be achieved by utilizing the implicit parallelization of multiple independent generations evolving simultaneously [46]. However, adapting the present GA for parallel distributed processing to improve its efficiency is out of the scope of the present study as the main purpose of the study is to show that a significantly higher active torsional vibration control effect can be achieved by performing a topology optimization of the collocated piezoelectric S/A pairs.

3. Genetic algorithm

The GA is a stochastic global search method based on the Darwinian survival-of-the-fittest principle to mimic the metaphor of natural biological evolution [43]. It operates on a population of potential solutions to produce better and better approximations to the optimal solution [44]. The population is a set of chromosomes and the basic GA operators are selection, crossover, and mutation. At each generation, a new set of approximations is created by the process of selecting individuals and breeding them together using crossover and mutation operators which are conceptually borrowed from natural genetics. Hopefully, this process leads to the evolution of populations of better individuals with respect to the global optimum [40]. Generally, the GA performs well in finding areas of interest even in a complex, real-world scene. However, in order that the GAs can be more generally applicable and effective, the GA operators must be chosen appropriately.

3.1. Chromosome representation

In the present study, the bit-array representation method, widely used by many researchers [40, 47–50], is adopted to define the topology of the S/A pairs, in which each discrete design variable can be either 0 or 1. This is a straightforward and natural representation method and the decoding step is almost eliminated [50].

3.2. Selection method

Selection is the process of determining the number of times that a particular individual is chosen for reproduction. In this study, the SUS (stochastic universal sampling) method [51] is adopted since SUS can ensure a selection closer to what is deserved than roulette wheel selection and has the advantage of minimizing chance fluctuations.

3.3. Crossover method

Crossover is the main GA operator to produce new individuals that have some parts of both parents' genetic material. The uniform crossover method [52] is adopted in the present work since it makes every locus a potential crossover point so that any form of associated bias is reduced.

3.4. Mutation method

Mutation is usually used as a background GA operator to enforce a random move in the neighborhood of a given point in the design domain. A binary mutation method in the breeder genetic algorithm (BGA) [53], which flips the value of each bit with a low mutation rate, is adopted to test more often in the neighborhood of the given point.

3.5. Evaluation of the fitness functions

In this study, Baker's linear ranking algorithm [54] with a selective pressure of 2 is used to ensure that no single individual generate an excessive number of offspring since rank-based fitness assignment usually behaves in a robust manner. The fitness of each individual in the population is defined as

$$\hat{F}(\boldsymbol{x}_i) = \frac{2\,(n_i - 1)}{N_{\text{ind}} - 1}, \tag{2}$$

where $\hat{F}(\boldsymbol{x}_i)$ is the fitness of the ith individual, n_i the position of the ith individual in the individuals' rank, and N_{ind} the population size.

3.6. Evaluation of the objective function

The structural topology optimization problem in equation (1) is a constrained optimization problem with a single objective and a few design constraints. Since the GA is a generic search method [55], most GA applications to constrained optimization problems have used the penalty function constraint handling approach to convert the constrained optimization problems into unconstrained optimization problems [55–58]. However, a major difficulty arises in how to set appropriate values for penalty parameters in order to obtain feasible best individuals in the population. To overcome this problem, a more efficient constraint handling approach is further developed based on Deb's method [55], which can be written as

$$F(\boldsymbol{x}) = \begin{cases} f(\boldsymbol{x}) & \text{if } \boldsymbol{x} \in \mathbb{F} \\ \tilde{f} + \text{viol}(\boldsymbol{x}) & \text{otherwise} \end{cases} \tag{3}$$

where $F(\boldsymbol{x})$ is the artificial unconstrained objective function, $\mathbb{F}$ the feasible solutions in the design domain Ω, $\tilde{f}$ the objective function value of the worst feasible solution in the

population, and viol($\boldsymbol{x}$) the summation of all the violated constraint function values. It can be seen from equation (3) that this approach is based on the penalty function approach, but it does not require any penalty parameter. Hence, it can be more efficient and robust. If there are no feasible individuals existing in the population, which is often seen in the early generations of the GA, a pre-defined worst value which can guarantee that any infeasible solution is worse than any feasible one, rather than 0 as recommended in Deb's method [55], is assigned to $\tilde{f}$ in order to allow the GA to use an elitist strategy. In Deb's method, since it is assumed $\tilde{f} = 0$ for this case, it cannot guarantee that any feasible solution is preferred to any infeasible solution when some most highly fit but infeasible individuals of the population are passed on to the next generation without being altered by genetic operators.

In the present study, the volume constraint introduced in the power-law approach by Sigmund in [33] is not necessary because materials cost for the small piezoelectric devices is low and some superfluous material may even have to be removed in manufacturing. On the other hand, in the power-law approach, as stated clearly in [33], without the volume constraint, there is a risk of ending up with final structures with large gray regions since the whole idea of the power-law approach would become lost. The introduction of this volume constraint not only increases the computational cost, but also makes the final solution dependent on the given value of the volume fraction and thus how to choose the volume fraction appropriately will become a new issue, which was not answered in [33]. In this study, it should also be noted that the voltage constraint for each S/A pair is not introduced because a negative velocity feedback control algorithm is used such that the magnitude of each actuator voltage can also be adjusted by the corresponding control gain [3].

The design connectivity analysis always plays a crucial role in structural topology optimization using the GAs and a bit-array representation method [47, 49, 50] since the design connectivity is always an active constraint and the bit-array representation itself cannot guarantee the design connectivity of the resulting topology. In the present study, the topology of each S/A pair must be well connected. It is assumed that the piezoelectric S/A pairs must be sparsely distributed, so the segmentation technique [20, 21], which requires that the piezoelectric materials cover the whole region continuously, cannot be used. Connectivity analysis based on the four-connected neighborhood assumption [40, 49] is adopted here. Figure 1 shows a topology with three connected objects, each of which is in accordance with the four-connected neighborhood assumption. Since edge connection is imposed for each connected S/A pair, the occurrence of checkerboard patterns can be prevented and thus the corresponding numerical instability can be overcome, different from the homogenization-based methods [32]. To deal with this connectivity issue in the framework of bit-array representation, the connectivity handling approach proposed by Wang and Tai [40] is further developed. For each feasible individual in the population, the total number of connected objects in the resulting topology must be the same as the given number of piezoelectric S/A pairs, or $n_c = n_\mathrm{p}$, where n_c is the total number of connected objects and n_p the pre-defined number of S/A pairs in the design domain Ω. If this

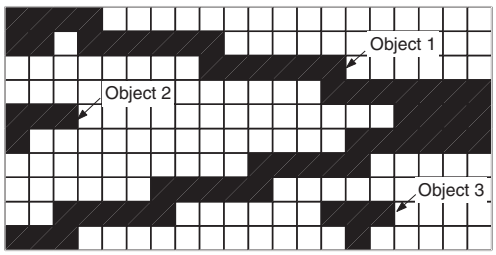

Figure 1. Connected objects in a design domain.

design connectivity constraint cannot be satisfied, viol($\boldsymbol{x}$) will be evaluated as follows:

$$\mathrm{viol}(\boldsymbol{x}) = \Gamma_c \, |n_c - n_\mathrm{p}| + \Gamma_\mathrm{m} \tilde{A}_\mathrm{m} \tag{4}$$

where Γ_c is the penalty multiplier for n_c connected objects of the topology and Γ_m the penalty multiplier for the object with a minimum area $\tilde{A}_\mathrm{m}$. This connectivity handling approach can be very efficient since the FE analysis step will be skipped if there is any connectivity constraint violation. It is well known that the FE analysis is the most time consuming part in GAs for structural topology optimization [40]. Different from the approach by Wang and Tai [40], $\tilde{A}_\mathrm{m}$ is added to overcome the problem of representation degeneracy [48] when different individuals have the same n_c but different $\tilde{A}_\mathrm{m}$, so that the connectivity handling approach can become robust. Less penalty on smaller $\tilde{A}_\mathrm{m}$ can also help eliminate the superfluous connected objects. Since the piezoelectric S/A pairs are assumed to be ideally bonded with the composite substrate, the requirement in [40] that $n_c = 1$ and the resulting topology be a load-bearing structure is not necessary in this study. Furthermore, the penalty on all the unusable objects in [40] is here removed since each separate object has the load-bearing capacity due to the perfect bonding and thus it is difficult to define unusable objects in this study. Although the values of those penalty multipliers are problem dependent in general, it should be guaranteed that $\Gamma_c \gg \Gamma_\mathrm{m} > 0$ such that the superfluous objects can be eliminated most effectively.

Hence, the original structural topology optimization problem in equation (1) becomes

$$\begin{aligned} &\max f(\boldsymbol{x}), \qquad \boldsymbol{x} \in \Omega \\ &\text{s.t.: } |n_c - n_\mathrm{p}| = 0. \end{aligned} \tag{5}$$

4. Active damping of torsional vibration control

4.1. Constitutive equations of piezoelectric composite plates

The linear constitutive relationship for the piezoelectric material [59] is adopted, which can be expressed as

$$\boldsymbol{\sigma} = \mathbf{C}\boldsymbol{\varepsilon} - \mathbf{e}^\mathrm{T}\mathbf{E}, \tag{6}$$

$$\mathbf{D} = \mathbf{e}\boldsymbol{\varepsilon} + \mathbf{g}\mathbf{E}, \tag{7}$$

where $\boldsymbol{\sigma}$ is the reduced stress vector ($\boldsymbol{\sigma} = [\sigma_x \ \sigma_y \ \sigma_{yz} \ \sigma_{zx} \ \sigma_{xy}]^\mathrm{T}$), $\mathbf{C}$ the transformed reduced elasticity matrix, $\boldsymbol{\varepsilon}$ the strain vector ($\boldsymbol{\varepsilon} = [\varepsilon_x \ \varepsilon_y \ \gamma_{yz} \ \gamma_{zx} \ \gamma_{xy}]^\mathrm{T}$), $\mathbf{e}$ the reduced piezoelectric constant matrix, $\mathbf{E}$ the electric field vector, $\mathbf{D}$

the electric displacement vector, and **g** the dielectric constant matrix [3]. Furthermore, the magnetically static electric field vector **E** is related to the electric potential field ϕ as follows [59]:

$$\mathbf{E} = -\nabla\phi. \tag{8}$$

For a piezoelectric composite laminate, based on equation (6) and the lamination theory and a perfect bonding assumption for the laminate [3], the converse constitutive equations can be written in matrix form as

$$\begin{Bmatrix} \mathbf{N} \\ \mathbf{M} \end{Bmatrix} = \begin{bmatrix} \mathbf{A} & \mathbf{B} \\ \mathbf{B}^{\mathrm{T}} & \mathbf{D} \end{bmatrix} \begin{Bmatrix} \boldsymbol{\varepsilon}^0 \\ \boldsymbol{\kappa}^0 \end{Bmatrix} - \begin{Bmatrix} \mathbf{N}^{\mathrm{p}} \\ \mathbf{M}^{\mathrm{p}} \end{Bmatrix} \tag{9}$$

where **N** and **M** are the force and moment resultants, respectively, **A** the extensional stiffness, **B** the coupling stiffness, **D** the bending stiffness, $\boldsymbol{\varepsilon}^0$ and $\boldsymbol{\kappa}^0$ the strains and curvatures of the mid-plane, respectively, $\mathbf{N}^{\mathrm{p}}$ and $\mathbf{M}^{\mathrm{p}}$ the equivalent force and moment resultants of the piezoelectric sensors/actuators, respectively, as defined in detail in [3].

4.2. Torsional vibration control

Since the plate under consideration is a thin composite laminate, the poling direction of the piezoelectric materials is in the thickness direction in which the external voltage can be applied. Generally, the through-the-thickness variation of the electric potential field is quite complicated [60]. Bisegna and Caruso [61] even suggested that it is necessary to take into account higher-order terms of up to the fourth order in the through-the-thickness electric potential representation in order to obtain accurate estimates of the stress and electric displacement fields. However, it should also be noted that usually the thickness of the piezoelectric layers is two to three orders less than that of the composite substrate [62]. Yang [63] has shown that the effect of a quadratic electric potential variation through the thick actuator thickness is negligible for thin actuators. The same conclusion has also been arrived at by Wang [60] using a layerwise-like through-the-thickness electric potential representation method. Therefore, the hypothesis first made by Mindlin [64] that the electric potential functions have only linear variations across the thickness of the piezoelectric layers is adopted in this study. Hence, for the ith piezoelectric layer, the electric field strength $\mathbf{E}_i$ can be written [3] as

$$\mathbf{E}_i = [\,0 \quad 0 \quad -V_i/h_i\,]^{\mathrm{T}} \tag{10}$$

where V_i is the electric voltage and h_i the thickness of the ith piezoelectric sensor/actuator.

It is well recognized that PZT is the most widely used among all the commercially available piezoelectric materials [11]. A PZT sensor/actuator is naturally isotropic in the plane of operation, i.e. $e_{31} = e_{32}$. Hence, we have $N^{\mathrm{p}}_{xy} = 0$, $M^{\mathrm{p}}_{xy} = 0$, which shows that it is impossible for an isotropic PZT actuator to provide twisting actuation directly [3]. Therefore, the torsional vibration cannot be directly suppressed through the twisting actuation of the PZT actuator. To overcome this problem, according to equation (9), the extension–twisting coupling of the composite laminate can be exploited. The constitutive equations for a piezoelectric angle-ply antisymmetric composite laminate can be simplified [3] as

$$\begin{Bmatrix} N_x \\ N_y \\ N_{yz} \\ N_{zx} \\ N_{xy} \\ M_x \\ M_y \\ M_{xy} \end{Bmatrix} = \begin{bmatrix} A_{11} & A_{12} & 0 & 0 & 0 & 0 & 0 & B_{16} \\ A_{12} & A_{22} & 0 & 0 & 0 & 0 & 0 & B_{26} \\ 0 & 0 & A_{44} & 0 & 0 & 0 & 0 & 0 \\ 0 & 0 & 0 & A_{55} & 0 & 0 & 0 & 0 \\ 0 & 0 & 0 & 0 & A_{66} & B_{16} & B_{26} & 0 \\ 0 & 0 & 0 & 0 & B_{16} & D_{11} & D_{12} & 0 \\ 0 & 0 & 0 & 0 & B_{26} & D_{12} & D_{22} & 0 \\ B_{16} & B_{26} & 0 & 0 & 0 & 0 & 0 & D_{66} \end{bmatrix} \times \begin{Bmatrix} \varepsilon^0_x \\ \varepsilon^0_y \\ \varepsilon^0_{yz} \\ \varepsilon^0_{zx} \\ \varepsilon^0_{xy} \\ \kappa^0_x \\ \kappa^0_y \\ \kappa^0_{xy} \end{Bmatrix} - \begin{Bmatrix} N^{\mathrm{p}}_x \\ N^{\mathrm{p}}_y \\ N^{\mathrm{p}}_{yz} \\ N^{\mathrm{p}}_{zx} \\ 0 \\ M^{\mathrm{p}}_x \\ M^{\mathrm{p}}_y \\ 0 \end{Bmatrix} \tag{11}$$

from which we have

$$M_{xy} = B_{16}\varepsilon^0_x + B_{26}\varepsilon^0_y + D_{66}\kappa^0_{xy}. \tag{12}$$

It can be seen that because of the existence of the extension–twisting coupling of the composite laminate ($B_{16} \neq 0$, $B_{26} \neq 0$) the torsional moment resultants M_{xy} are coupled with the extensional strains, which can be directly suppressed by the PZT actuator ($N^{\mathrm{p}}_x \neq 0$, $N^{\mathrm{p}}_y \neq 0$). Hence, the torsional vibration can be indirectly damped out. However, if a piezoelectric cross-ply asymmetric composite laminate is used, the constitutive equations will be changed [3] as

$$\begin{Bmatrix} N_x \\ N_y \\ N_{yz} \\ N_{zx} \\ N_{xy} \\ M_x \\ M_y \\ M_{xy} \end{Bmatrix} = \begin{bmatrix} A_{11} & A_{12} & 0 & 0 & 0 & B_{11} & 0 & 0 \\ A_{12} & A_{22} & 0 & 0 & 0 & 0 & -B_{11} & 0 \\ 0 & 0 & A_{44} & 0 & 0 & 0 & 0 & 0 \\ 0 & 0 & 0 & A_{55} & 0 & 0 & 0 & 0 \\ 0 & 0 & 0 & 0 & A_{66} & 0 & 0 & 0 \\ B_{11} & 0 & 0 & 0 & 0 & D_{11} & D_{12} & 0 \\ 0 & -B_{11} & 0 & 0 & 0 & D_{12} & D_{22} & 0 \\ 0 & 0 & 0 & 0 & 0 & 0 & 0 & D_{66} \end{bmatrix}$$

$$\times \begin{Bmatrix} \varepsilon_x^0 \\ \varepsilon_y^0 \\ \varepsilon_{yz}^0 \\ \varepsilon_{zx}^0 \\ \varepsilon_{xy}^0 \\ \kappa_x^0 \\ \kappa_y^0 \\ \kappa_{xy}^0 \end{Bmatrix} - \begin{Bmatrix} N_x^{\mathrm{p}} \\ N_y^{\mathrm{p}} \\ N_{yz}^{\mathrm{p}} \\ N_{zx}^{\mathrm{p}} \\ 0 \\ M_x^{\mathrm{p}} \\ M_y^{\mathrm{p}} \\ 0 \end{Bmatrix} \tag{13}$$

from which we have

$$M_{xy} = D_{66}\kappa_{xy}^0 \tag{14}$$

which shows that the torsional moment resultant of a cross-ply asymmetric composite laminate is not influenced by the piezoelectric effects. Therefore, isotropic PZT actuators cannot be used for torsional vibration control of a cross-ply composite laminate. If anisotropic PZT actuators are used, the equivalent shear stress τ_{xy}^{p} of an anisotropic piezoelectric actuator with an applied voltage of V_{p} and a thickness of h_{p} can be written [3] as

$$\tau_{xy}^{\mathrm{p}} = \sin\theta\cos\theta(e_{32} - e_{31})V_{\mathrm{p}}/h_{\mathrm{p}} \tag{15}$$

where θ is the skew angle of the piezoelectric material. Since $e_{32} \neq e_{31}$, it can be inferred that τ_{xy}^{p}, as well as N_{xy}^{p} and M_{xy}^{p}, will be non-zero and thus the torsional vibration can be directly suppressed.

It should be noted that there are some other methods in the literature to damp out the torsional vibration [8, 11]. Aldraihem and Wetherhold [11] developed an anisotropic composite actuator (the PZT/Ep composite) to suppress the torsional vibration directly. Rogers and Hagood [8] used active fiber composite (AFC), which is actually made of PZT fibers. In the present study, only isotropic and anisotropic PZT sensors/actuators are considered.

4.3. Evaluation of the active damping effect

By using Hamilton's variational principle [22], Wang *et al* [3, 35] derived the governing equations of motion of the piezoelectric composite plate in terms of the global coordinates with the standard procedure of the FE method as follows:

$$\mathbf{M}_{uu}\ddot{\tilde{\mathbf{U}}} + \mathbf{K}_0\tilde{\mathbf{U}} = \mathbf{F} + \mathbf{K}_{ua}\tilde{\boldsymbol{\Phi}}_{\mathrm{a}}, \tag{16}$$

where $\tilde{\mathbf{U}}$ and $\tilde{\boldsymbol{\Phi}}_{\mathrm{a}}$ are the global coordinates representing the global generalized mechanical displacements and the global electric potentials of the piezoelectric actuators, respectively, $\mathbf{M}_{uu}$ the consistent mass matrix, $\mathbf{K}_0$ the generalized stiffness matrix, $\mathbf{K}_{ua}$ the electromechanical coupling matrix of the piezoelectric actuators, and $\mathbf{F}$ the external mechanical forces [3].

Based on the charge output of the piezoelectric electroplated sensors, a negative-velocity feedback control system can be established [3, 35] as

$$\tilde{\boldsymbol{\Phi}}_{\mathrm{a}} = -\mathbf{G}\,\boldsymbol{\Phi}_{\mathrm{s}}, \tag{17}$$

in which $\mathbf{G}$ is the constant gain matrix (usually diagonal), Φ_{s} is the sensor output, which can be obtained in an alternative way by using the charge output $\mathbf{Q}_{\mathrm{s}}$ of each electroplated sensor [3, 22, 23, 35].

The governing equations of motion (16) in the absence of exogenous disturbance and the sensor equation [3] can be transformed into the first-order linear state space form as

$$\dot{\mathbf{x}} = \bar{\mathbf{A}}\mathbf{x} + \bar{\mathbf{B}}\mathbf{u}, \tag{18}$$

$$\mathbf{y} = \bar{\mathbf{C}}\mathbf{x}, \tag{19}$$

where $\mathbf{x} = [\tilde{\mathbf{U}} \quad \dot{\tilde{\mathbf{U}}}]^{\mathrm{T}}$ is the state variable vector, $\mathbf{y} = \boldsymbol{\Phi}_{\mathrm{s}}$ the output voltage vector, $\mathbf{u} = \tilde{\boldsymbol{\Phi}}_{\mathrm{a}}$ the actuator input voltage vector, $\bar{\mathbf{A}}$ the system matrix, $\bar{\mathbf{B}}$ the input matrix, and $\bar{\mathbf{C}}$ the output matrix [3]. Hence, equation (18) can be re-written as

$$\dot{\mathbf{x}} = (\bar{\mathbf{A}} - \bar{\mathbf{B}}\mathbf{G}\bar{\mathbf{C}})\mathbf{x} \tag{20}$$

and thus a characteristic equation is obtained as follows:

$$|\lambda\mathbf{I} - (\bar{\mathbf{A}} - \bar{\mathbf{B}}\mathbf{G}\bar{\mathbf{C}})| = 0, \tag{21}$$

to which the solution λ is the complex eigenvalue of the asymmetric matrix $(\bar{\mathbf{A}} - \bar{\mathbf{B}}\mathbf{G}\bar{\mathbf{C}})$, which can be expressed as

$$\lambda = \mu + \mathrm{i}\,\omega_{\mathrm{d}}. \tag{22}$$

Correspondingly, the damping ratio ζ can be defined to be the negative of the normalized real part of the complex eigenvalue λ [22] as

$$\zeta = -\frac{\mu}{\sqrt{\mu^2 + \omega_{\mathrm{d}}^2}}. \tag{23}$$

In the present study, it is assumed that the passive structural damping effect can be ignored. Hence, the damping ratio of the torsional vibration mode under consideration can be used to measure the active damping effect, which can be expressed as

$$f(\boldsymbol{x}) = \zeta_i, \tag{24}$$

where ζ_i is the damping ratio of the torsional mode.

In order to find the time response solution to the first order equation (20), the state transition matrix method [65] is employed. The time response of the state vector $\mathbf{x}$ at the $(k+1)$th step can be obtained by utilizing the information at the kth step as follows:

$$\mathbf{x}((k+1)T) = \boldsymbol{\Psi}((k+1)T, kT)\mathbf{x}(kT) \tag{25}$$

where T is the sampling period and $\boldsymbol{\Psi}$ the state transition matrix given by

$$\boldsymbol{\Psi}(t,\ \tau) = \mathrm{e}^{(\bar{\mathbf{A}} - \bar{\mathbf{B}}\mathbf{G}\bar{\mathbf{C}})(t-\tau)}. \tag{26}$$

5. Numerical results and discussion

Two numerical examples are used in this study. The first one is to find the optimal topology of conventional materials for a minimum compliance design problem to verify the present GA. The second one is to find the optimal topology of smart PZT materials to suppress the torsional vibration most effectively.

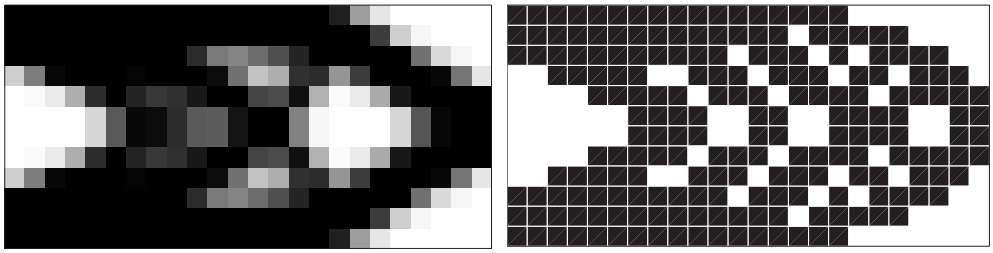

(a) Power-law approach (b) Present GA

Figure 2. Optimal topology of the 2 × 1 clamped beam.

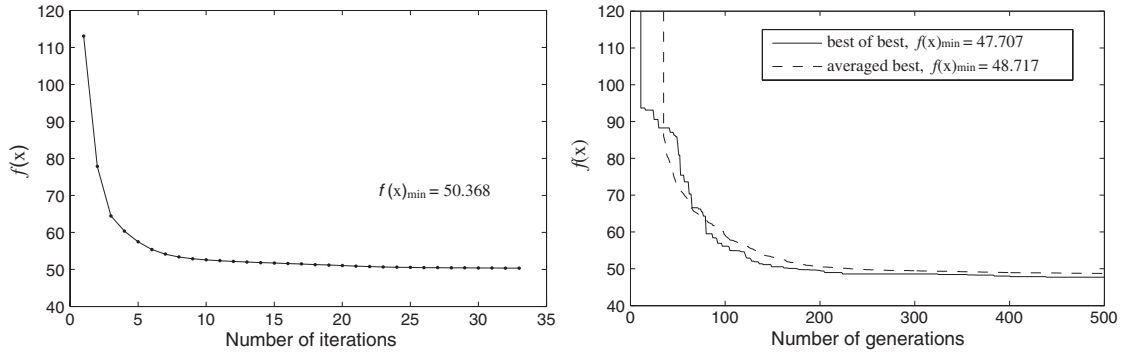

(a) Power-law approach (b) Present GA

Figure 3. Convergence of the objective function for the 2 × 1 clamped beam.

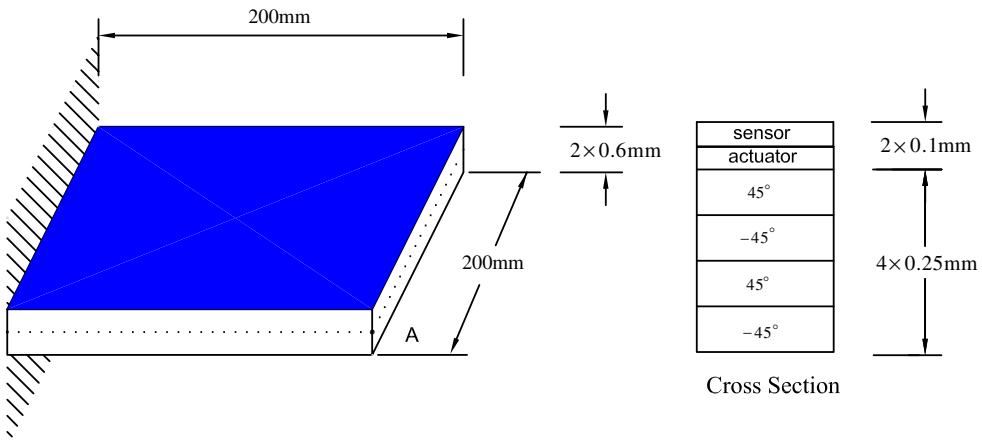

Figure 4. The geometry of a piezoelectric composite plate.

5.1. Minimum compliance design

This example will demonstrate the performance of the present GA in dealing with the minimum compliance design problem [29] of a clamped beam with a volume fraction of 0.7, a symmetric design domain of the size $2H \times H$ ($H = 5$) discretized into a 24 × 12 mesh and a unit point force applied vertically downward at half-height of the right boundary [40]. As aforementioned, the FE model in [3, 35] used for the present GA is an eight-noded isoparametric quadratic element and can thus be more accurate than the usually adopted four-noded bi-linear rectangular element [29]. Furthermore, as stated by Bendsøe and Sigmund [32], using a relatively coarse mesh can also give a good indication of the optimal topology. Hence, for illustrative purposes only, a relatively coarse mesh is used for the relatively simple examples in the present study. The basic parameters are assumed to be $E = 1.0$, $\nu = 0.3$, density $\rho = 1.0$, thickness $t = 1.0$. The GA is a standard simple GA with a population size of 100, a generation gap of 0.9, a mutation rate of 0.01, and an elitist strategy to keep the fittest individuals. 21 independent GA runs have been carried out and all runs are stopped after 500 generations.

The final optimal topology obtained from the present GA is compared in figure 2 with the one obtained from the power-law approach using the MATLAB code from Sigmund [29].

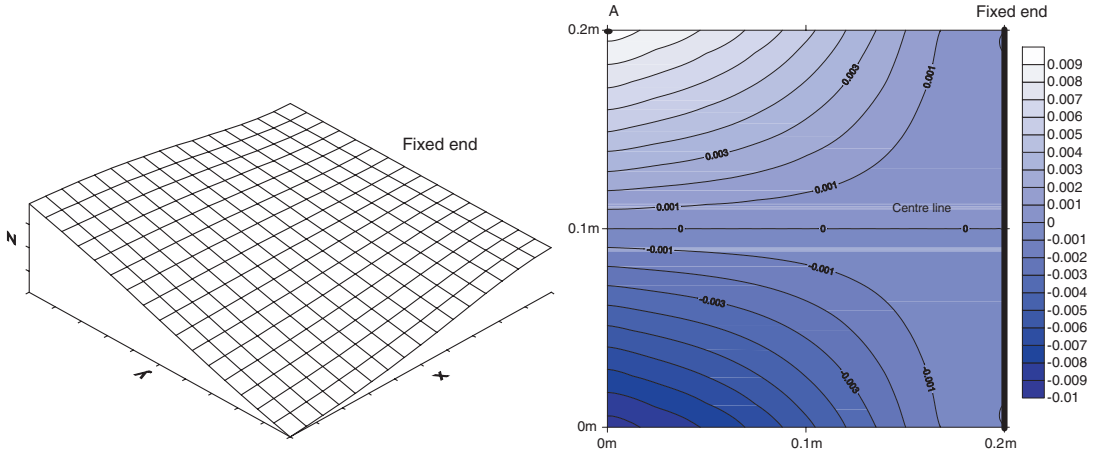

(a) Mode shape (b) Contour map

Figure 5. The torsional mode.

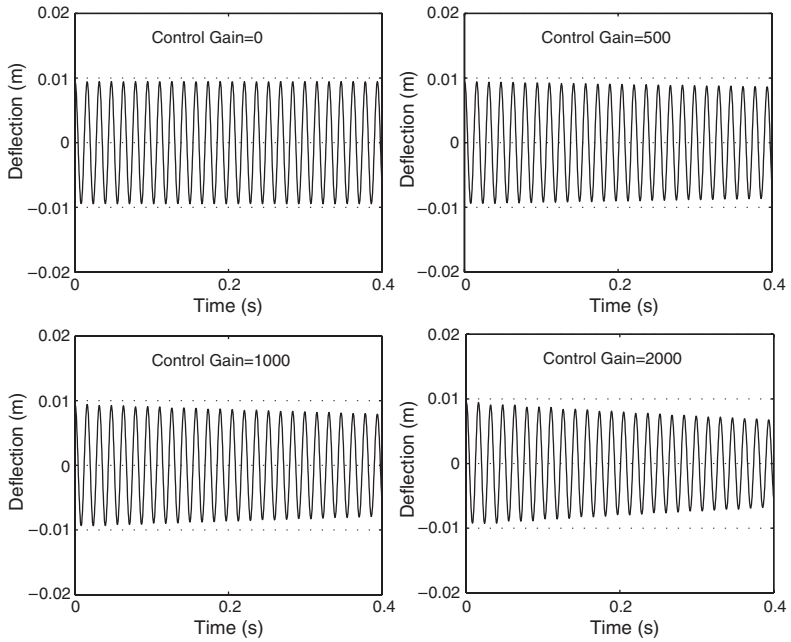

Figure 6. Time history of the deflection of corner point A (angle-ply substrate).

As expected, the power-law approach gives a blurry boundary while the present GA produces a black-and-white design with a clear definition of both the interior and exterior boundaries. It can also be seen that the boundaries of the final optimal topology are jagged since the FE mesh of the structural analysis model is kept unchanged throughout the optimization process, which is commonly adopted in topology optimization [66], different from some placement optimization methods [67], in which moving mesh templates and remeshing techniques are used. It should be noted that remeshing is a source of numerical noise that could ultimately take over the actual difference in mechanical behavior between two very similar structures [56]. Further comparison on the convergence speed is shown in figure 3. The present GA converges to a better solution than the power-law approach because the former is a global search method while the latter is only a local search method. It can also be seen that the present GA converges much more slowly than the power-law approach. This is the typical difference between a local optimization method and a global optimization method, as mentioned in [25]. For some real world problems only the best (extremum) is good enough and therefore a global optimization method has to be applied. Actually, global optimization problems are widespread in the mathematical modeling of real world systems for a broad range of applications. It should also be noted that the enumeration method for 0–1 global optimization problems cannot be used here since the search space for this example would be as large as $2^{24\times12} = 4.97 \times 10^{86}$ and thus it requires formidable computation. Hence the present GA is a practical alternative

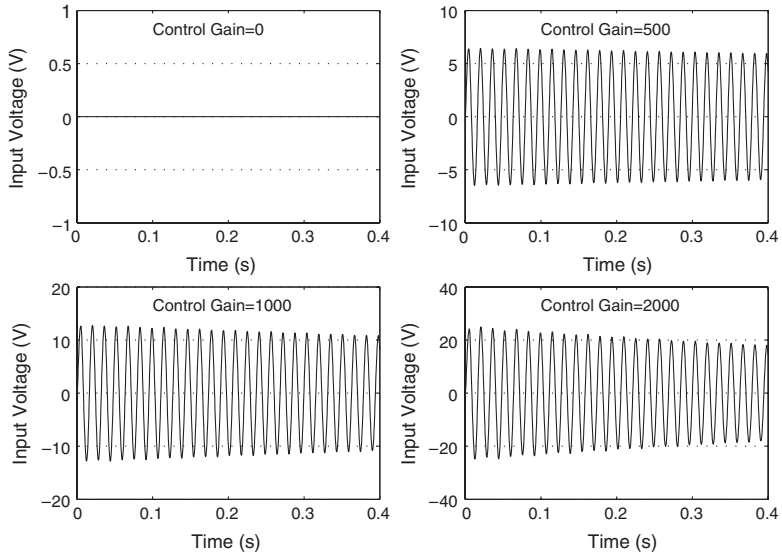

Figure 7. Time history of the input voltage of the isotropic PZT actuator (angle-ply substrate).

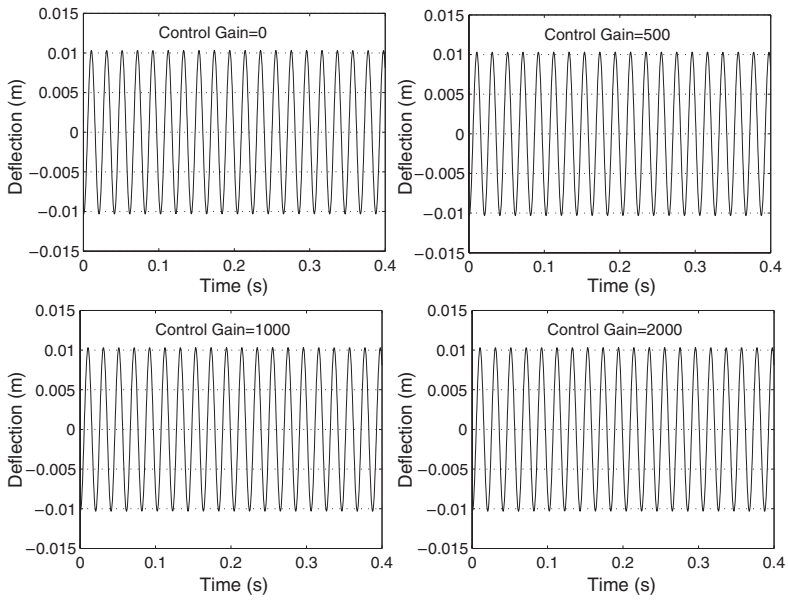

Figure 8. Time history of the deflection of corner point *A* (cross-ply substrate).

to the (global) enumeration method due to the size of the search space.

5.2. Torsional vibration control

This example will demonstrate the efficiency of topology optimization of piezoelectric S/A pairs for torsional vibration control. As shown in figure 4, a cantilevered piezoelectric composite plate is adopted, which consists of four composite substrate layers and two outer PZT layers bonded at the top surface of the composite substrate serving as sensor and actuator, respectively. The stacking sequence of the composite substrate is antisymmetric angle-ply $[45^\circ/-45^\circ/45^\circ/-45^\circ]$. The substrate is made of T300/976 graphite–epoxy composite, the piezoelectric layers are made of either isotropic PZT G1195N or anisotropic PZT5A fiber composite and their corresponding material properties are listed in table 1. The following settings are used in the numerical experiments of the GA presented below: standard SGA evolution with a population size of 20, a fraction of 0.1 of the population are considered elites and a generation gap of 0.9 and a mutation rate of 0.01; all runs are stopped after 100 generations; all the runs are carried out using MATLAB based on a mesh of 8×8; and all the results obtained for each problem are based on 20 independent runs of the GA.

The torsional mode under consideration, which is the second mode of the composite plate, is shown in figure 5(a), where the mode shape is normalized as $\|\boldsymbol{X}\| = 1$, in which $\boldsymbol{X}$ is the modal displacement vector. As shown in figure 5(b), the centerline of the plate approximately does not bend after

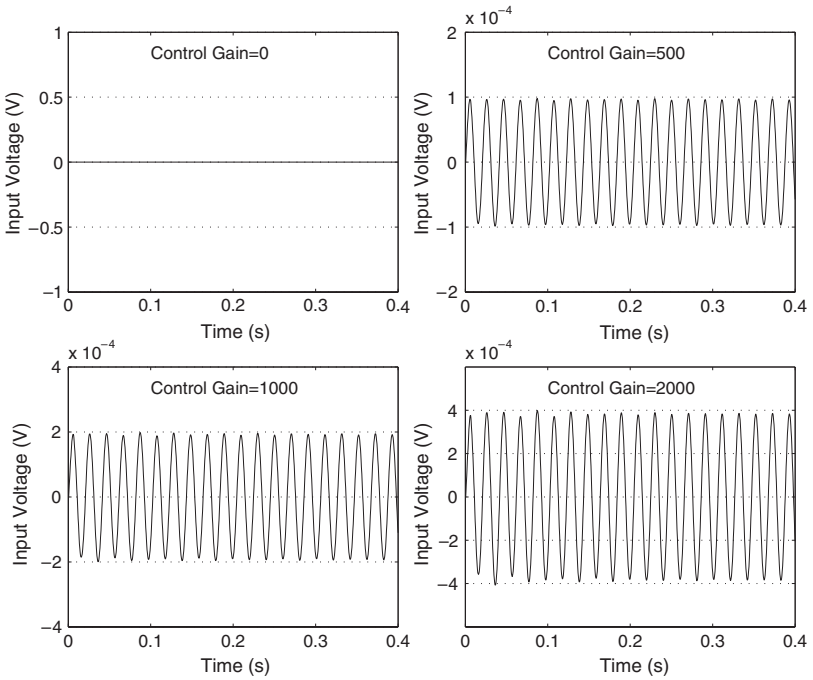

Figure 9. Time history of the input voltage of the isotropic PZT actuator (cross-ply substrate).

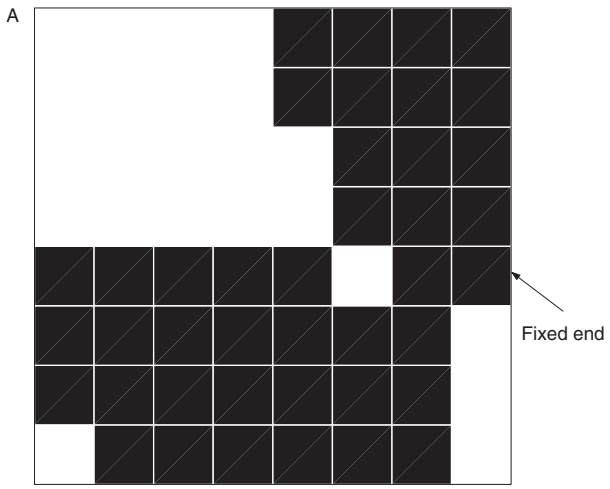

Figure 10. Optimal topology of a single isotropic PZT S/A pair.

deformation for this torsional mode. It is assumed that the torsional vibration is excited by a suddenly removed load and the structural passive damping effect can be ignored. In the present study, this torsional vibration mode is damped out by using the isotropic or anisotropic PZT S/A pairs and the optimal topologies of the PZT S/A pairs are obtained from the present GA.

5.2.1. Isotropic PZT S/A pairs. The isotropic PZT S/A pairs are made of the PZT G1195N. The special case where a PZT S/A pair covers the whole top surface of the composite plate continuously, which was often adopted by many researchers [11, 14, 22, 35, 68], is first studied. Figures 6 and 7 show the history of the decay of the deflection of the

Table 1. Material properties of the composite lamina and piezo-ceramics.

Material	T300/976	PZT G1195N	PZT5A fiber composite
E_{11} (GPa)	150	63	30.2
E_{22} (GPa)	9	63	14.9
G_{12} (GPa)	7.1	24.2	5.13
G_{23} (GPa)	2.5	24.2	5.13
ν_{12} (GPa)	0.3	0.3	0.45
ρ (kg m^{-3})	1600	7600	4060
d_{31} (pm V^{-1})	—	−254	309
d_{32} (pm V^{-1})	—	−254	−129
ϵ_{11} (F m^{-1})	—	15.3×10^{-9}	8.3×10^{-9}
ϵ_{22} (F m^{-1})	—	15.3×10^{-9}	6.8×10^{-9}
ϵ_{33} (F m^{-1})	—	15.0×10^{-9}	6.1×10^{-9}

corner point A and the input voltage of the PZT actuator, respectively. It can be seen that the torsional vibration can be damped out, and the higher the control gain the faster the speed of decay but the higher the input voltage of the PZT actuator. The reason is that, according to equation (11), the torsional vibration can be damped out by exploiting the extension–twisting coupling of this antisymmetric composite laminate. It also shows that if the control gain is zero, the torsional vibration cannot be suppressed since the input voltage will also be zero, according to equation (17). Although the torsional vibration can be damped out, it is not answered whether this configuration of a PZT S/A pair is an efficient one or not.

To further verify the present algorithm on vibration control simulation, another special case where the composite substrate is changed to be cross-ply asymmetric [0°/90°/0°/90°] is also studied and the corresponding responses are shown in figures 8 and 9. It can be seen that the torsional vibration cannot be suppressed for this case because, according to

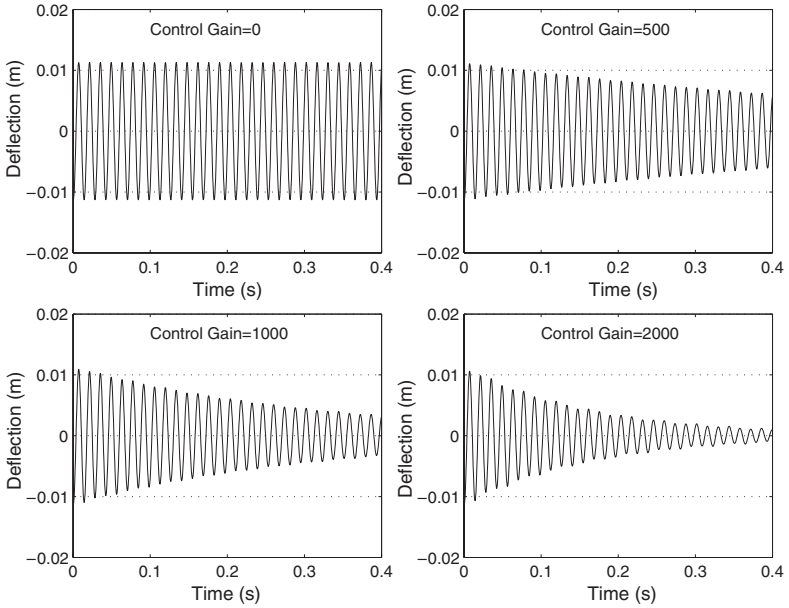

Figure 11. Time history of the deflection of corner point *A* (optimal solution).

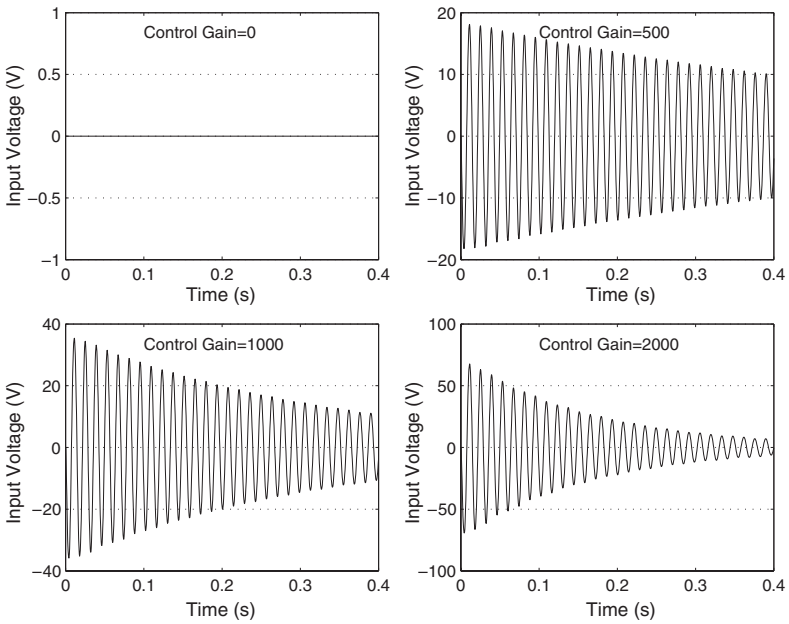

Figure 12. Time history of the input voltage of the isotropic PZT actuator (optimal solution).

equation (13), the isotropic PZT actuator cannot provide either a direct twisting actuation or an indirect one through the coupling effect, as mentioned above. Hence, good agreement between numerical results and the theoretical prediction has been achieved.

The present GA is applied to topology optimization of the isotropic PZT S/A pair for torsional vibration control of the angle-ply antisymmetric composite plate. Figure 10 shows the optimal topology of a single PZT S/A pair, while figures 11 and 12 show the history of the decay of the deflection of the corner point *A* and the input voltage of the PZT actuator, respectively. It can be seen that the damping effect and control voltage will increase with the control gain. All the shown highest control voltages under different control gains are well below the breakdown voltage, which is approximately 100 V for this example [3]. Comparing figure 11 with 6, it can be seen that topology optimization of the PZT S/A pair can improve the damping effect significantly. Table 2 shows the active damping ratios obtained for two different configurations of the PZT S/A pairs. The active damping effect obtained by using the optimal topology can be up to six times better than the one by using the S/A pair covering the whole top surface continuously. Hence, topology optimization is quite attractive even though the material cost for PZT applications in small

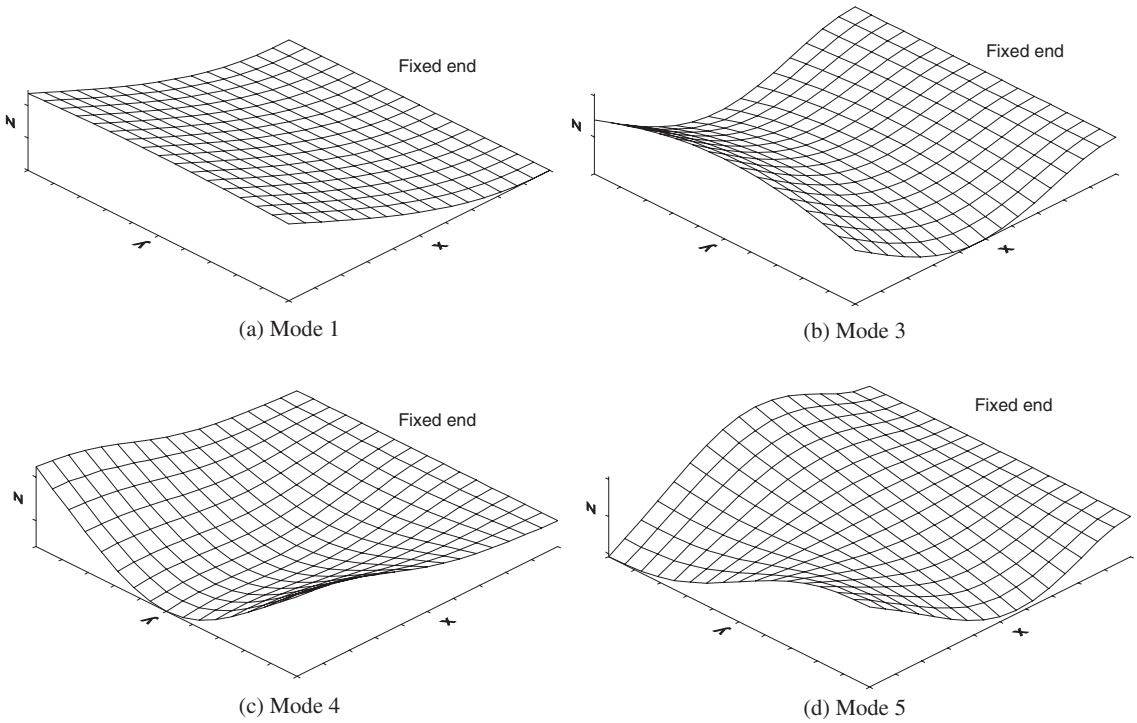

Figure 13. The first few modes.

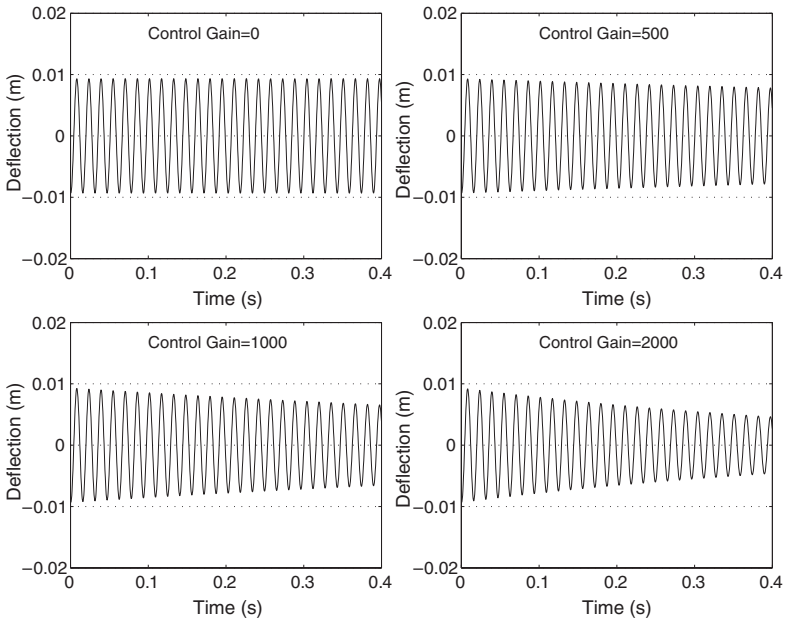

Figure 14. Time history of the deflection of corner point *A* (optimal skew angle only).

devices is low. Furthermore, the optimal volume fraction for this topology optimization of a single S/A pair is 64% and thus more material may not improve the damping effect. As discussed in detail in [30], if the PZT S/A pair is continuously distributed in the whole design domain, since there are both positive and negative mechanical strains existing in this design domain, the sensing and actuation effects of the PZT pair, which are dependent on the integration of the mechanical strains, will not be maximized and thus the active damping effect cannot be maximized. This is totally different from the minimum compliance structural design problems, in which higher volume fraction will generate better objective function value [32] and thus the optimal volume fraction will be unity if no volume constraint is prescribed. The effect of the optimal topological design of the PZT S/A on the active damping effect of the first few modes is also studied. Figures 13 and 5(a)

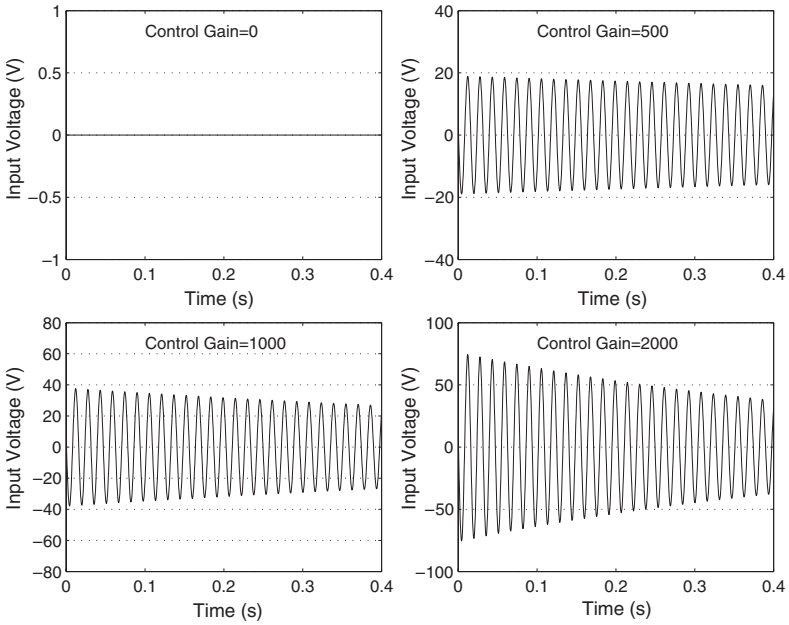

Figure 15. Time history of the input voltage of the anisotropic PZT actuator (optimal skew angle only).

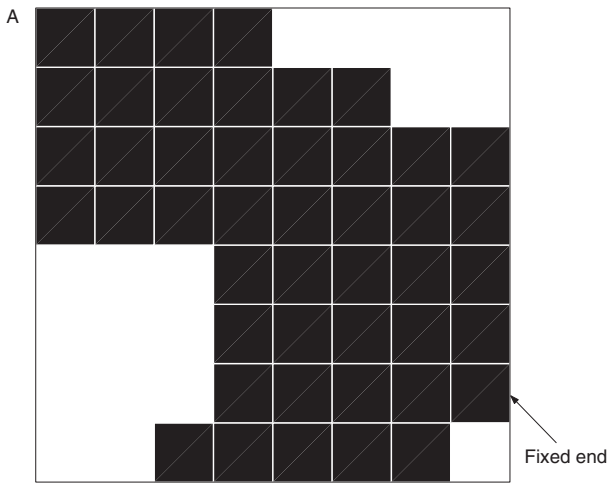

Figure 16. Optimal topology of a single anisotropic PZT S/A pair.

Table 2. Active damping ratios for different configurations of the isotropic PZT S/A pair.

Control gain	0	500	1000	2000
PZT covering the whole surface	0	0.0006	0.001	0.002
PZT with optimal topology	0	0.003	0.007	0.014

Table 3. Active damping ratios for the first five modes using the isotropic PZT S/A pair.

Control gain	500	1000	2000
Mode 1	3.62×10^{-3}	7.24×10^{-3}	1.44×10^{-2}
Mode 2	3.49×10^{-3}	6.93×10^{-3}	1.36×10^{-2}
Mode 3	4.93×10^{-4}	9.68×10^{-4}	1.79×10^{-3}
Mode 4	9.69×10^{-3}	1.88×10^{-2}	3.35×10^{-2}
Mode 5	1.16×10^{-3}	2.29×10^{-3}	4.45×10^{-3}

display the shapes of the first five modes and table 3 lists the corresponding active damping ratios. It can be seen that the first five modes can all be damped out, though the topology is designed to suppress the torsional mode (mode 2) most effectively. Hence, this optimal design is robust in this sense.

5.2.2. Anisotropic PZT S/A pair. The anisotropic PZT S/A pairs are made of the PZT5A fiber composite, which consists of isotropic PZT fibers [8]. The special case where a single PZT S/A pair covers the whole top surface of the composite plate continuously is first studied. The optimal skew angle of the anisotropic PZT pair for this case is obtained by using the present GA. The final solution of this optimal skew angle is $\theta = -57.15°$ and the corresponding responses are shown in figures 14 and 15. Comparing figure 14 with figure 6, it can be seen that when the PZT pair is continuously distributed in the whole design domain, the anisotropic PZT pair with an optimal skew angle can damp out the torsional vibration more effectively than the isotropic one since the former can provide a direct twisting actuation, as shown in equation (15).

The optimal topology of the PZT S/A pair as well as the corresponding skew angle can also be obtained by using the present GA. Figure 16 shows the optimal topology (optimal skew angle $\theta = -45.65°$ and optimal volume fraction 72%), while figures 17 and 18 show the corresponding responses. Again, it can be seen that the torsional vibration can be damped out and the speed of decay increases with the control gain. Comparing figure 17 with figure 14, it can be seen that the anisotropic PZT with optimal topology can damp out the torsional vibration more effectively. Table 4 lists the active damping ratios for this torsional mode. The active damping effect obtained by using this optimal topology can be up to 1.5 times better than the one by using the S/A pair continuously distributed in the whole design domain.

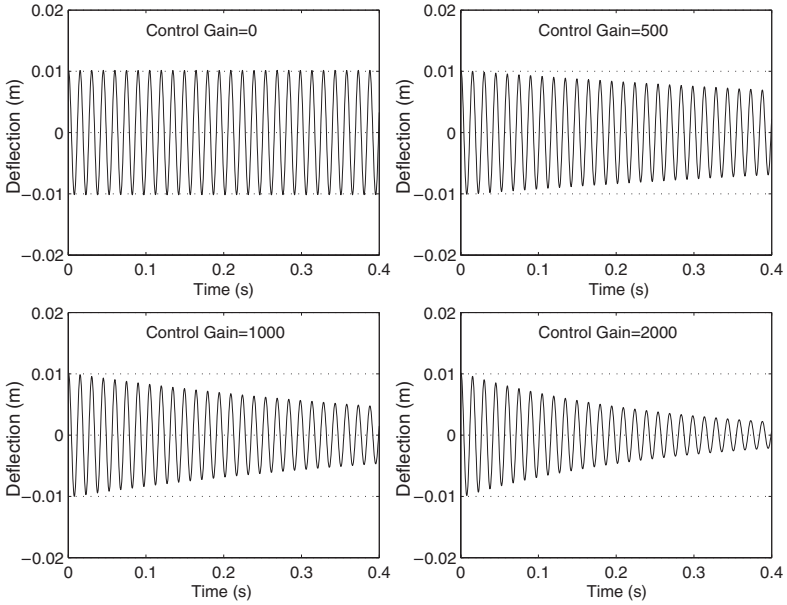

Figure 17. Time history of the deflection of corner point A (optimal solution).

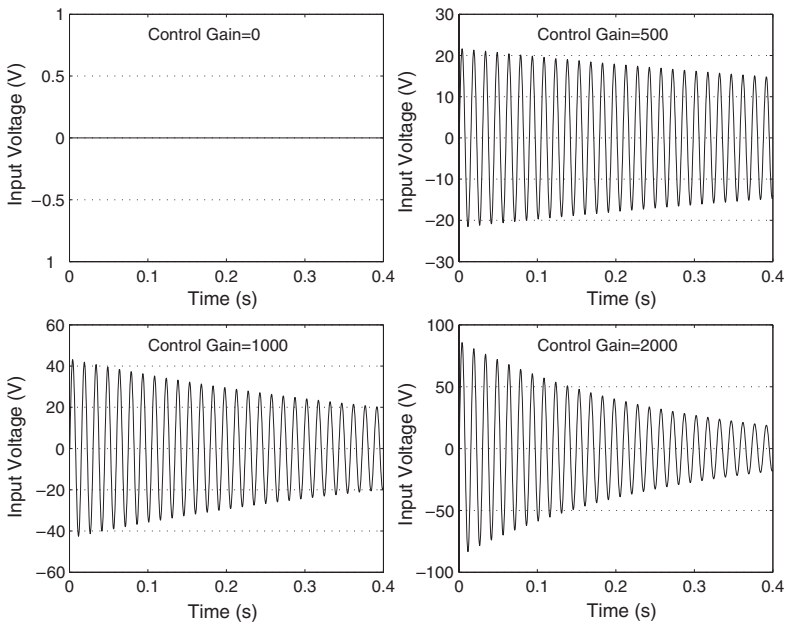

Figure 18. Time history of the input voltage of the anisotropic PZT actuator (optimal solution).

Table 4. Active damping ratios for different configuration of the anisotropic PZT S/A pair.

Control gain	0	500	1000	2000
PZT covering the whole surface	0	0.001	0.002	0.004
PZT with optimal topology	0	0.002	0.005	0.009

Comparing the active damping ratios listed in table 4 with those listed in table 2, it can be seen that the isotropic PZT with optimal topology damps out the torsional vibration more effectively than the anisotropic one (up to 56% higher in the active damping ratio). The reason may be that the isotropic PZT has much higher elastic constants (about twice as high in E_{11}) and larger dielectric constants (about 2.4 times higher in e_{31}) such that the extension–twisting coupling effect can be greatly enhanced.

6. Conclusions

Topology optimization of piezoelectric S/A pairs for torsional vibration control of a laminated composite plate is investigated by using an improved bit-array representation GA and a finite element model based on the first-order shear theory and an output feedback control law. Both the isotropic

and anisotropic PZT S/A pairs are used for damping out the torsional vibration by exploiting either the extension–twisting coupling of the antisymmetric composite laminate or the direct twisting actuation of anisotropic PZT composites. The bit-array representation GA is further improved by using a more effective constraint handling approach, which guarantees that feasible individuals be preferred to infeasible ones, and a design connectivity handling approach, which prevents the occurrence of the checkerboard pattern and improves the computational efficiency. The torsional vibration can be damped out more effectively by using the topology optimization of the piezoelectric sensor/actuator pairs since both the distributed sensing and actuation effects can be maximized. Numerical examples show that compared with the PZT pair continuously distributed in the whole design domain, the PZT pair with optimal topology can achieve significantly better active damping effect (up to sixfold for the isotropic PZT and 1.5-fold for the anisotropic PZT). It is thus suggested that topology optimization of piezoelectric materials for active vibration control is effective and rewarding. Further developments on the present topology optimization methods for simultaneous optimal design of the structure, sensors/actuators, electronics, and control system, as well as the extensions to three-dimensional optimal topological design for more general vibration control problems using the powerful parallel and distributed computation techniques, are the fields for future research.

References

[1] Reddy J N 1997 *Mechanics of Laminated Composite Plates: Theory and Analysis* (Boca Raton, FL: CRC Press)

[2] Matthews F L, Davies G A O, Hitchingsand D and Soutis C 2000 *Finite Element Modeling of Composite Materials and Structures* (Cambridge: Woodhead)

[3] Wang S Y 2002 Active vibration control of smart piezoelectric composite plates *PhD Dissertation* National University of Singapore

[4] Mackerle J 2003 Smart materials and structures—a finite element approach—an addendum: a bibliography (1997–2002) *Modelling Simul. Mater. Sci. Eng.* **11** 707–44

[5] Frecker M I 2003 Recent advances in optimization of smart structures and actuators *J. Intell. Mater. Syst. Struct.* **14** 207–16

[6] Fernandes A and Pouget J 2003 Analytical and numerical approaches to piezoelectric bimorph *Int. J. Solids Struct.* **40** 4331–52

[7] Wang S Y, Quek S T and Ang K K 2004 Dynamic stability analysis of finite element modeling of piezoelectric composite plates *Int. J. Solids Struct.* **41** 745–64

[8] Rodgers J P and Hagood N W 1998 Preliminary Mach-scale hover testing of an integral twist-actuated rotor blade *SPIE Smart Structures and Materials Conf. (San Diego, CA)* (*Proc. SPIE* vol 3329) ed M E Regelbrugge (Bellingham, WA: SPIE Optical Engineering Press)

[9] Lee C K 1987 Piezoelectric laminates for torsional and bending modal control: theory and experiment *PhD Dissertation* Cornell University

[10] Lee C K 1990 Theory of laminated piezoelectric plates for the design of distributed sensors/actuators. Part I: governing equations and reciprocal relationships *J. Acoust. Soc. Am.* **87** 1144–58

[11] Aldraihem O J and Wetherhold R C 1997 Mechanics and control of coupled bending and twisting vibration of laminated beams *Smart Mater. Struct.* **6** 123–33

[12] Park C, Walz C and Chopra I 1996 Bending and torsion models of beams with induced-strain actuators *Smart Mater. Struct.* **5** 98–113

[13] Lee S W R and Chan K H W 1995 Actuation of torsional motion for piezoelectric laminated beams *Proc. ASME WAM* vol 5, ed C T Sun (New York: ASME) pp 139–46

[14] Zhu M L, Lee S W R, Li H L, Zhang T Y and Tong P 2002 Modeling of torsional vibration induced by extension-twisting coupling of anisotropic composite laminates with piezoelectric actuators *Smart Mater. Struct.* **11** 55–62

[15] Lee S W R and Li H L 1998 Development and characterization of a rotary motor driven by anisotropic piezoelectric composite laminate *Smart Mater. Struct.* **7** 327–36

[16] Rabinovitch O and Vinson J R 2003 On the design of piezoelectric smart fins for flight vehicles *Smart Mater. Struct.* **12** 686–95

[17] Padula S L and Kincaid R K 1999 Optimization strategies for sensors and actuators placement *Report* NASA/TM-1999-209126 *National Aeronautics and Space Administration Langley Research, Langley, Virginia 23681, USA*

[18] Buehler M J, Bettig B and Parker G G 2004 Topology optimization of smart structures using a homogenization approach *J. Intell. Mater. Syst. Struct.* **15** 655–67

[19] Burke S and Hubbard J E 1987 Active vibration control of a simply supported beam using a spatially distributed actuator *IEEE Control Syst. Mag.* **7** 25–30

[20] Tzou H S and Fu H Q 1994 A study of segmentation of distributed piezoelectric sensors and actuators, Part I: theoretical analysis *J. Sound Vib.* **172** 247–59

[21] Han J H and Lee I 1999 Optimal placement of piezoelectric sensors and actuators for vibration control of a composite plate using genetic algorithms *Smart Mater. Struct.* **8** 257–67

[22] Hwang W S and Park H C 1993 Finite element modeling of piezoelectric sensors and actuators *AIAA J.* **31** 930–7

[23] Hwang W S, Hwang W and Park H C 1994 Vibration control of laminated composite plate with piezoelectric sensor/actuator: active and passive control methods *Mech. Syst. Signal Process.* **8** 571–83

[24] Silva E C N and Kikuchi N 1999 Design of piezoelectric transducers using topology optimization *Smart Mater. Struct.* **8** 350–64

[25] Rozvany G I N 2001 Aims, scope, methods, history and unified terminology of computer-aided topology optimization in structural mechanics *Struct. Multidisciplinary Optim.* **21** 90–108

[26] Li Y, Xin X, Kikuchi N and Saitou K 2001 Optimal shape and location of piezoelectric materials for topology optimisation of flextensional actuators *GECCO-2001: Proc. Genetic and Evolutionary Computation Conf.* ed L Spector *et al* (San Francisco, CA: Morgan Kaufmann) pp 1085–90

[27] Zhu Y, Qiu J, Du H and Tani J 2002 Simultaneous optimal design of structural topology, actuator locations and control parameters for a plate structure *Comput. Mech.* **29** 89–97

[28] Bendsøe M P 1989 Optimal shape design as a material distribution problem *Struct. Optim.* **1** 193–202

[29] Sigmund O 2001 A 99 line topology optimization code written in MATLAB *Struct. Multidisciplinary Optim.* **21** 120–27

[30] Quek S T, Wang S Y and Ang K K 2003 Vibration control of composite plates via optimal placement of piezoelectric patches *J. Intell. Mater. Syst. Struct.* **14** 229–46

[31] Sigmund O and Torquato S 1999 Design of smart composite materials using topology optimization *Smart Mater. Struct.* **8** 365–79

[32] Bendsøe M P and Sigmund O 2003 *Topology Optimization: Theory, Methods and Applications* (Berlin: Springer)

[33] Sigmund O 2001 Design of multiphysics actuators using topology optimization. Part I: one material structures *Comput. Methods Appl. Mech. Eng.* **190** 6577–604
[34] Li K, Zeng D W, Yung K C, Chan H L W and Choy C L 2002 Study on ceramic/polymer composite fabricated by laser cutting *Mater. Chem. Phys.* **75** 147–50
[35] Wang S Y, Quek S T and Ang K K 2001 Vibration control of smart piezoelectric composite plates *Smart Mater. Struct.* **10** 637–44
[36] Bendsøe M P and Sigmund O 1999 Material interpolations in topology optimization *Arch. Appl. Mech.* **69** 635–54
[37] Bendsøe M P and Kikuchi N 1988 Generating optimal topologies in structural design using a homogenization method *Comput. Methods Appl. Mech. Eng.* **71** 197–224
[38] Stolpe M and Svanberg K 2001 On the trajectories of penalization methods for topology optimization *Struct. Multidisciplinary Optim.* **21** 128–39
[39] Wang S Y and Tai K 2004 Graph representation for structural topology optimization using genetic algorithms *Comput. Struct.* **82** 1609–22
[40] Wang S Y and Tai K 2005 Structural topology design optimization using genetic algorithms with a bit-array representation *Comput. Methods Appl. Mech. Eng.* **194** 3749–70
[41] Wang M Y and Wang S Y 2005 Bilateral filtering for structural topology optimization *Int. J. Numer. Methods Eng.* **63** 1911–38
[42] Wang S Y, Tai K and Wang M Y 2006 An enhanced genetic algorithm for structural topology optimization *Int. J. Numer. Methods Eng.* **65** 18–44
[43] Holland J 1975 *Adaptation in Natural and Artificial Systems* (Ann Arbor, MI: University of Michigan Press)
[44] Goldberg D E 1989 *Genetic Algorithms in Search, Optimization and Machine Learning* (Reading, MA: Addison-Wesley)
[45] Stolpe M and Svanberg K 2003 Modelling topology optimization problems as linear mixed 0–1 programs *Int. J. Numer. Methods Eng.* **57** 723–39
[46] Cantu-Paz E 2000 *Efficient and Accurate Parallel Genetic Algorithms* (Boston, MA: Kluwer–Academic)
[47] Chapman D, Saitou K and Jakiela M J 1994 Genetic algorithms as an approach to configuration and topology design *J. Mech. Design* **116** 1005–12
[48] Schoenauer M 1996 Shape representations and evolutionary schemes *Evolutionary Programming: Proc. 5th Annual Conf. on Evolutionary Programming (San Diego, USA)* pp 121–9
[49] Jakiela M J, Chapman C, Duda J, Adewuya A and Saitou K 2000 Continuum structural topology design with genetic algorithms *Comput. Methods Appl. Mech. Eng.* **186** 339–56
[50] Fanjoy D W and Crossley W A 2002 Topology design of planar cross-sections with a genetic algorithm: part 1—overcoming the obstacles *Eng. Optim.* **34** 1–12
[51] Baker J E 1987 Reducing bias and inefficiency in the selection algorithm *Proc. 2nd Int. Conf. on Genetic Algorithms* ed J J Grefenstette (Cambridge, MA: Lawrence Erlbaum Associates) pp 14–21
[52] Spears W M and De Jong K A 1991 On the virtues of parameterized uniform crossover *Proc. 4th Int. Conf. on Genetic Algorithms* ed R Belew and L Booker (San Mateo, CA: Morgan Kaufman) pp 230–6
[53] Mühlenbein H and Schlierkamp-Voosen D 1994 The science of breeding and its application to the breeder genetic algorithm (BGA) *Evol. Comput.* **1** 335–60
[54] Baker J E 1985 Adaptive selection methods for genetic algorithms *Proc. Int. Conf. on Genetic Algorithms and Their Applications* ed J J Grefenstette (Pittsburgh, PA: Lawrence Erlbaum Associates) pp 101–11
[55] Deb K 2000 An efficient constraint handling method for genetic algorithms *Comput. Methods Appl. Mech. Eng.* **186** 311–38
[56] Hamda H, Jouve F, Lutton E, Schoenauer M and Sebag M 2002 Compact unstructured representations for evolutionary design *Appl. Intell.* **16** 139–55
[57] Kane C and Schoenauer M 1996 Topological optimum design using genetic algorithms *Control Cybern.* **25** 1059–88
[58] Lagaros N D, Papadrakakis M and Kokossalakis G 2002 Structural optimization using evolutionary algorithms *Comput. Struct.* **80** 571–89
[59] Tzou H S and Tseng C I 1990 Distributed piezoelectric sensor/actuator design for dynamic measurement/control of distributed parameter systems: a piezoelectric finite element approach *J. Sound Vib.* **138** 17–34
[60] Wang S Y 2004 A finite element model for the static and dynamic analysis of a piezoelectric bimorph *Int. J. Solids Struct.* **41** 4075–96
[61] Bisegna P and Caruso G 2001 Evaluations of higher-order theories of piezoelectric plates in bending and in stretching *Int. J. Solids Struct.* **38** 8805–30
[62] Samanta B, Ray M C and Bhattacharyya R 1996 Finite element model for active control of intelligent structures *AIAA J.* **34** 1885–93
[63] Yang J S 1999 Equations for thick elastic plates with partially electroded piezoelectric actuators and higher order electric fields *Smart Mater. Struct.* **8** 73–82
[64] Mindlin R D 1972 High frequency vibrations of piezoelectric crystal plates *Int. J. Solids Struct.* **8** 895–906
[65] Kwon Y W and Bang H 1997 *The Finite Element Method Using MATLAB* (Boca Raton, FL: CRC Press)
[66] Hammer V B and Olhoff N 2000 Topology optimization of continuum structures subjected to pressure loading *Struct. Multidisciplinary Optim.* **19** 85–92
[67] Varadan V V, Kim J and Varadan V K 1997 Optimal placement of piezoelectric actuators for active noise control *AIAA J.* **35** 526–33
[68] Tzou H S 1993 Piezoelectric shells *Solid Mechanics and its Applications* vol 19 (Dordrecht: Kluwer–Academic)